RESEARCH ARTICLE

WILEY

Decreasing distance from tumor to the language network causes language deficit

Shengyu Fang[1,2] | Shimeng Weng[2] | Lianwang Li[2] | Yuhao Guo[2] | Zhong Zhang[1] | Xing Fan[2] | Tao Jiang[1,2,3] (ORCID) | Yinyan Wang[1,2]

[1]Department of Neurosurgery, Beijing Tiantan Hospital, Capital Medical University, Beijing, China

[2]Beijing Neurosurgical Institute, Capital Medical University, Beijing, China

[3]Research Unit of Accurate Diagnosis, Treatment, and Translational Medicine of Brain Tumors, Chinese Academy of Medical Sciences, Beijing, China

Correspondence
Xing Fan, Tao Jiang, Yinyan Wang, Department of Neurosurgery, Beijing Tiantan Hospital, Capital Medical University, 119, The Western Road of the southern 4th Ring Road, Beijing, China.
Email: xingkongyaoxiang@163.com, taojiang1964@foxmail.com, and tiantanyinyan@126.com

Abstract

Preoperative language deficits are associated with alterations in the language networks of patients with gliomas. This study investigated how gliomas affect language performance by altering the language network. Ninety patients with lower-grade gliomas were included, and their preoperative language performance was evaluated using the Western Aphasia Battery. We also calculated the topological properties based on resting state functional magnetic resonance imaging. All patients were classified according to aphasia quotient (AQ) into the aphasia (AQ < 93.8), mild anomia (AQ > 93.8 and naming section <9.8), and normal groups (AQ > 93.8). The shortest distance from the tumor to the language network (SDTN) was evaluated to identify the effect on language performance induced by the tumor. One-way analysis of variance and post hoc analysis with Sidak correction were used to analyze the differences in topological properties among the three groups. Causal mediation analysis was used to identify indirectly affected mediators. Compared with the mild anomia group, longer shortest path length ($p = .0016$), lower vulnerability ($p = .0331$), and weaker nodal efficiencies of three nodes (right caudal Brodmann area [BA] 45, right caudal BA 22, and left BA 41/42, all $p < .05$) were observed in the aphasia group. The SDTN mediated nodal degree centrality and nodal vulnerability (left rostroventral BA 39), which negatively affected the AQs. Conventional language eloquent and mirrored areas participated in the language network alterations induced by gliomas. The SDTN was a mediator that affected the preoperative language status in patients with gliomas.

KEYWORDS
gliomas, language deficits, language network, resting state functional magnetic resonance, topological theory

---

Shengyu Fang and Shimeng Weng contributed equally to this work.

1 | INTRODUCTION

Language deficit is a common neurological symptom in patients with gliomas (Zhang et al., 2021). Preoperative language deficit is reportedly associated with abnormal alterations in language network (Yuan et al., 2019; Zhang et al., 2021). However, not all patients experience language deficit when the gliomas invade close to language-related eloquent areas (Plaza et al., 2009; Satoer et al., 2014). This discrepancy in language performance suggests that glioma-induced impairment may be compensated in some patients owing to the plasticity and reorganization of brain networks (Duffau, 2014). In addition, language reorganization induced by gliomas has been reported in bilateral hemispheres based on task blood oxygen level-dependent (BOLD) functional magnetic resonance imaging (fMRI) (Cirillo et al., 2019). Nevertheless, identifying how the bilateral hemisphere cortices compensate for damaged language functions (i.e., recognizing reorganized patterns in language networks) using task BOLD fMRI is difficult.

Alterations in brain networks can be quantitatively delineated based on functional connectivity (FC) and topological properties (Chen et al., 2022; Fang, Zhou, et al., 2021), which are two types of indices originating from resting state fMRI (rs-fMRI). The relationship between language deficits and alterations in FC has been previously well described (Briganti et al., 2012; Cho et al., 2022). However, the FC only reflected alterations in synchronicity between two nodes (Biswal et al., 1995) and did not reflect the connective hierarchy of all nodes in one network (Liu et al., 2008). Hence, identifying the contribution of each node in an entire whole network during task performance is crucial for investigating the topological properties (de Lange et al., 2019).

Limited studies investigated the relationship between language deficit and topological properties in patients with gliomas. Some previous studies have reported decreased language network efficiency and that patients with stroke and accompanying language deficit were vulnerable (Chen et al., 2022; Forkel et al., 2014; Zhu et al., 2016). However, unlike stroke, glioma is a progressive tumor that results in the recruitment of adjacent and contralesional cortices to reorganize the disrupted networks in order to compensate for damaged functions (Fang, Liang, et al., 2021; Satoer et al., 2014). Hence, previous conclusions based on patients with stroke may not be applicable to patients with gliomas. Thus, an investigation of how the alterations of topological properties in the language network are related to language deficits induced by gliomas is needed (the details of each are provided in table S1).

In this study, we aimed to investigate how gliomas alter the language network and which alterations result in preoperative language deficit.

2 | MATERIALS AND METHODS

2.1 | Patients

A total of 115 patients diagnosed with grade II or III gliomas between September 2018 and January 2022 at the Beijing Tiantan Hospital were included in this study. The inclusion criteria were as follows: (1) age > 18 years and (2) a primary diagnosis of glioma. The exclusion criteria were as follows: (1) brain midline shift and (2) head rotation over $1°$ or head motion over 1 mm. Written informed consent was obtained from all patients, and our institutional review board approved the study.

2.2 | Language assessment

The Western Aphasia Battery (WAB) was used to evaluate the preoperative language status of each patient within 24 h before tumor resection. The aphasia quotient (AQ = [fluency + comprehension/20 + repetition/10 + naming/10] × 2) was calculated from the WAB and used to evaluate language performance. Patients were first sorted into aphasia (AQ < 93.8) and nonaphasia (AQ > 93.8) groups. Moreover, naming function is one of the main cognitive functions that is at risk of decline when language impairment occurs (Clark et al., 2020). Hence, if the naming function score was <9.8 (detailed information regarding the naming score determination threshold is shown in the supplementary methods Part 1) (Kertesz, 1974), patients in the nonaphasia group were considered to have impaired naming function and were classified into the mild anomia (MA) group. Otherwise, the patients were classified into the normal group. The postoperative AQs were obtained between days 7 and 10 after tumor resection.

2.3 | Awake craniotomy procedure

All patients underwent awake craniotomy and language mapping with direct cortical bipolar stimulators (Ojemann, Integra Radionics, Inc., Burlington, MA, USA; bipolar interval distance = 5 mm). The awake craniotomy and language mapping procedures were performed as described in our previous study (Fang, Liang, et al., 2021). During the intraoperative monitoring procedure, the patient performed a picture-naming task in Chinese for language mapping (http://cgga.org.cn/language_test/index.jsp). If the stimulation of a site caused speech arrest, anomia, dysarthria, or slowing of speech, the site was labeled as a potential positive site. If at least two stimulations (2/3 principle) in a same site caused positive reactions, the site was defined as a positive site. Subsequently, sterile circles with a 5-mm diameter were used to mark each positive site. Moreover, we acquired the central point of each sterile circle using an intraoperative neuro-navigation system (BrainLab®, Brainlab AG, Munich, Germany).

After language mapping of the cortex with the patient in an awake state, tumor removal was initiated while avoiding the parts at positive sites. Direct cortical stimulation was applied to the sub-cortices during language mapping to identify the language-related fibers before continuing with deep tumor removal.

2.4 | MRI acquisition

Using a MAGNETOM Prisma 3 T MR scanner (Siemens, Erlangen, Germany), all MR images were acquired within 24 h before surgery.

T1-magnetization prepared rapid acquisition gradient echo was applied to collect anatomical images (flip angle: 8°; repetition time [TR]: 2300 ms; echo time [TE]: 2.3 ms; field of view [FOV]: 240 × 240 mm^2; voxel size: 1.0 × 1.0 × 1.0 mm^3; slice number: 192). T2-weighted sequences were used to acquire glioma images (flip angle: 150°; TR: 5000 ms; TE: 105 ms; FOV: 240 × 240 mm^2; voxel size: 0.5 × 0.5 × 3 mm^3; slice number: 33). Finally, an echo-planar imaging sequence was applied for rs-fMRI (flip angle: 75°; TR: 2000 ms; TE: 30 ms; FOV: 220 × 220 mm^2; voxel size: 3.0 × 3.0 × 5.0 mm^3; slice number: 30; acquisition duration: 8 min; patients were instructed to remain relaxed and not think about anything during the scanning).

2.5 | Rs-fMRI data preprocessing

Theoretical network analysis software (GRaph thEoreTical Network Analysis [GRETNA], https://www.nitrc.org/projects/gretna) was used to preprocess the rs-fMRI data. The preprocessing pipeline was performed as previously described (Fang, Wang, et al., 2021; Fang et al., 2020). The sequential steps included converting data, removing initial images, slice timing, reorientation, normalization, smoothing, temporal detrending, covariance regression, temporal filtering, and scrubbing.

The rs-fMRI data were processed as follows: (a) transformation to a NIFTI file, (b) removal of the first five time points, (c) slice timing, (d) realignment, (e) normalization to echo-planar imaging template (Calhoun et al., 2017), (f) smoothing (full width half maximum = 4 mm), (g) temporal detrending (linear detrending), (h) covariance regression (white matter signal: with WMMask_3mm; CSF signal: with CSFMask_3mm; head motion: Friston-24 parameters), (i) temporal filtering (0.01–0.08 Hz), and (j) scrubbing (linear interpolation, subsequent time point number: 2; FD threshold: 0.5; and previous time point number: 1).

2.6 | Regions of interest

The language network was extracted from a brain atlas known as "brant 274" (Brainnetome Center, Beijing, China; http://www.brainnetome.org/) comprised of 28 nodes located in the Broca's and Wernicke's areas, the mirror sides of these two areas, and bilateral mouth motor areas (Fan et al., 2016). Detailed information for each region of interest (ROI) is provided in Table S2. Based on the coordinates, each ROI was generated as a ball with a diameter of 5 mm.

Notably, the rs-fMRI analysis may have been affected by the glioma itself. To minimize the image signal bias, the positive language mapping sites from the direct cortical stimulation results during the awake craniotomy were used to replace the nodes that were occupied by the tumor (Tuncer et al., 2021) based on the markers in the intraoperative photos and positive points acquired using the neuronavigation system. By using MRIcron software, the positive points were transformed to the sphere with a diameter of 5 mm. Then, the newly generated ROIs were registered to the standard echo-planar

imaging template using SPM8 toolbox. Eventually, corresponding template of language network for each patient was created to calculate FC matrix in the further step based on the new ROI and the rest of language network (excluding the invaded ROI). In this study, there were five patients who had ROIs invaded by the tumor and replaced by the new node (the specific instructions for individuals were reported in Figure 1 and Figure S1, S2, S3, S4).

2.7 | Regions of lesion

Based on the region of high signals on T2 fluid-attenuated inversion recovery, the extent of glioma occupation was manually and independently drawn by one of the authors who has more than 10 years of clinical experience, with consensus from another senior neurosurgeon. Eventually, all tumor masks were normalized into the standard space of the T2 template (i.e., the Montreal Neurological Institute template) using SPM8 software (The Wellcome Centre for Human Neuroimaging, UCL Queen Square Institute of Neurology, London, UK; http://www.fil.ion.ucl.ac.uk/spm/software/spm8/). A volumetric method was applied to calculate the tumor volume using MRIcron software (http://www.mccauslandcenter.sc.edu/mricro/mricron/) according to the tumor masks.

2.8 | Functional connectivity construction and topological properties calculation

By using the mean time series between the two ROIs using Pearson's correlation, the FC matrix was constructed by 28 nodes and 378 connections/edges. Subsequently, each matrix was transformed into a Z-score. The FC matrices were compared pairwise among the three groups, total of 1134 (378*3) times.

Global and nodal properties were calculated based on positive and weighted FC matrices using GRETNA software. The sparsity series ranged from 0.10 to 0.40 with an interval of 0.01.

2.9 | Statistical analysis

All statistical analyses were performed using SPSS software, version 19.0 (IBM Corp., Armonk, NY, USA); GraphPad Prism software, version 8.0 (GraphPad Software, San Diego, CA, USA); and PROCESS, version 3.0 by Hayes.

According to the type of data, differences in general clinical information among the three groups were determined using Chi-square and one-way analysis of variance (ANOVA) tests. Differences in FC matrices and topological properties among the three groups were determined using one-way ANOVA. The difference was considered statistically significant when p was <.05, and post hoc analysis with Sidak correction was applied.

Pearson's correlation was used to analyze the correlation between AQs and topological properties in patients ($n = 49$) in the
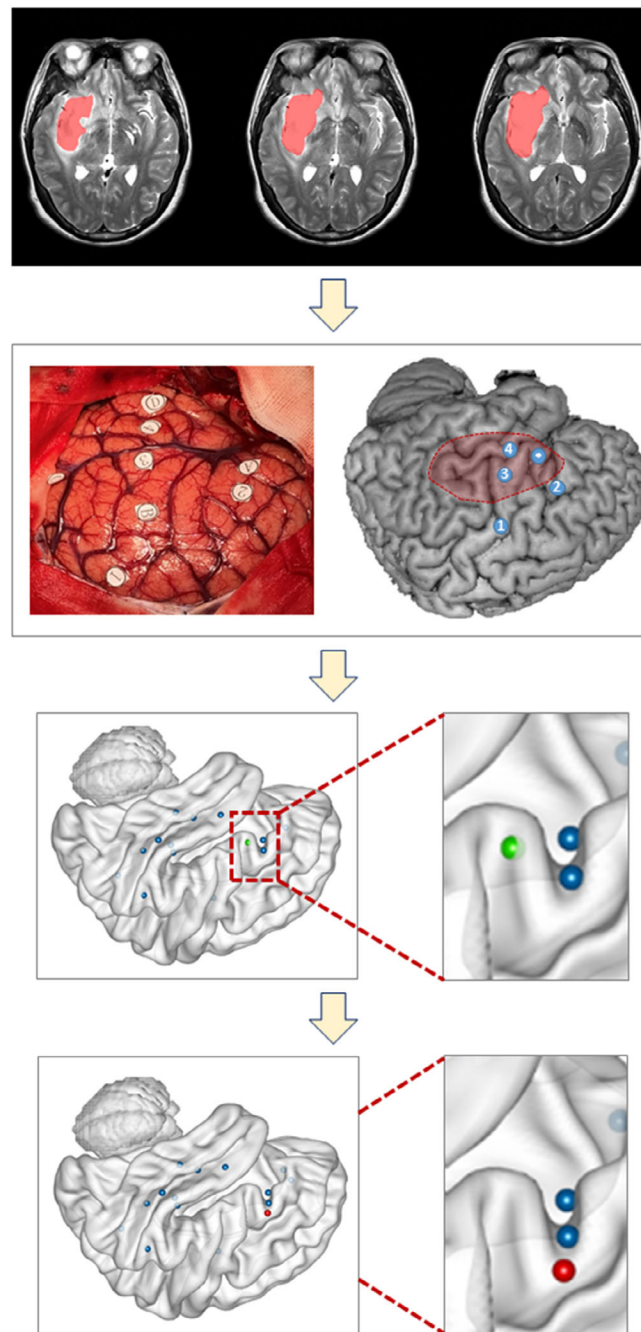
FIGURE 1 Results of ROI replacement in patient No. 5. The first panel shows the tumor location; the red region is the tumor. The second panel shows the intraoperative photo and examples of positive points. The blue asterisk indicates that the region of interest (ROI) was on the language template and invaded by glioma. Moreover, the blue circles with numbers 2–4 represent positive sites that presented with speech arrest during language mapping, and the blue circle with number 1 represents mouth movement during motor mapping. The green ball in third panel represents the blue ball with asterisk in the second panel. Furthermore, the red ball in the lowest panel represents the blue ball with No. 2 in the second panel, which was the closest positive language site to the invaded ROI with similar language function. Therefore, the blue ball with No. 2 was chosen as the new ROI to replace the blue asterisk (green ball)

aphasia and MA groups. Moreover, causal mediation analysis (model number: 4; confidence interval: 95%; number of bootstraps: 5000) was used to detect the factors that influence different outcomes of language impairment.

The shortest distance between the tumor and the language network (SDTN; Figure 2) was calculated based on the coordinates of ROI and the point located on the tumor border using the following formula, in which the ROI coordinates for point R are represented by
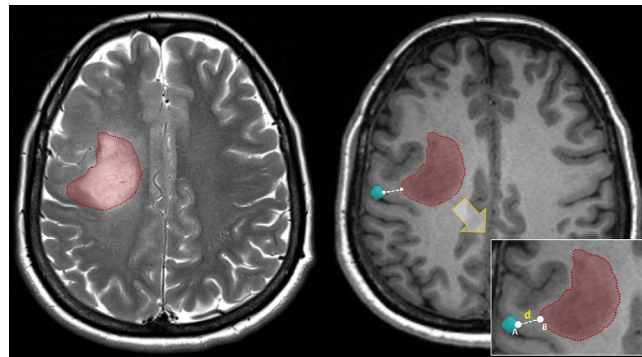
FIGURE 2 The shortest distance from the tumor to the language network (SDTN). The left panel was T2-weighted image and the region of high signal represents the glioma (red region). The right panel was T1-3D image and the red region was the same as in the left panel and represented the glioma. The blue region represented a node of the language network that was left hemispheric Brodmann area 4 (A4hf, head and face region). This node was nearest to the glioma for this patient. The point A and point B were the points that respectively located on the node A4hf and the glioma. The dotted white line (d) represented the shortest distance that was calculated based on the coordinates of the point A and point B

TABLE 1 Demographic and tumor characteristics of patients

Demographic and clinical characteristics	Aphasia (*n* = 21)	MA (*n* = 28)	Normal (*n* = 41)	*p* value
Sex				.982
Male	11	15	21	
Female	10	13	20	
Age (y)[a]	46.8 ± 2.3	43.1 ± 2.0	40.4 ± 1.7	.097
Education Level (y)[a]	11.4 ± 0.9	12.0 ± 0.6	13.4 ± 0.5	.074
AQ	88.2 ± 1.7	98.6 ± 0.1	100.0	<.001
Naming score	8.7 ± 0.1	9.3 ± 0.1	10.0	<.001
Post-AQ	55.0 ± 5.7	83.8 ± 4.2	91.2 ± 3.1	<.001
Post-naming score	5.8 ± 0.7	7.6 ± 0.6	8.8 ± 0.4	.001
Tumor volume (mL)[a]	32.78 ± 4.81	28.99 ± 3.34	26.52 ± 3.29	.529
Tumor location				.320
Frontal	12	13	23	
Temporal	3	1	4	
Parietal	4	9	9	
Insular	0	2	1	
Insular – temporal	1	0	0	
Insular – frontal	0	1	4	
Insular–frontal–temporal	1	2	0	
SDTN (mm)[a]	5.83 ± 0.30	12.10 ± 1.10	16.91 ± 1.59	<.001
IDH status				.293
Mutation	14	23	34	
Wild-type	7	5	7	
Chromosome 1p/19q status				.883
Co-deletion	8	11	18	
Noncodeletion	13	17	23	

Note: MA, the group of patients with mild anomia; AQ, Aphasia quotient score; SDTN, the shortest distance from the tumor to the language network; IDH, isocitrate dehydrogenase; chromosome 1p/19q, the short arm chromosome 1 and the long arm of chromosome 19. One-way Analysis of Variance was used to compare age, education level, AQ, naming score, postnaming score, tumor volume, and SDTN between the three groups. Kruskal-Walls test was used to compare post AQ between the three groups. Chi-square tests were used to compare sex, tumor location, IDH status, and chromosome 1p/19q co-deletion between the three groups.
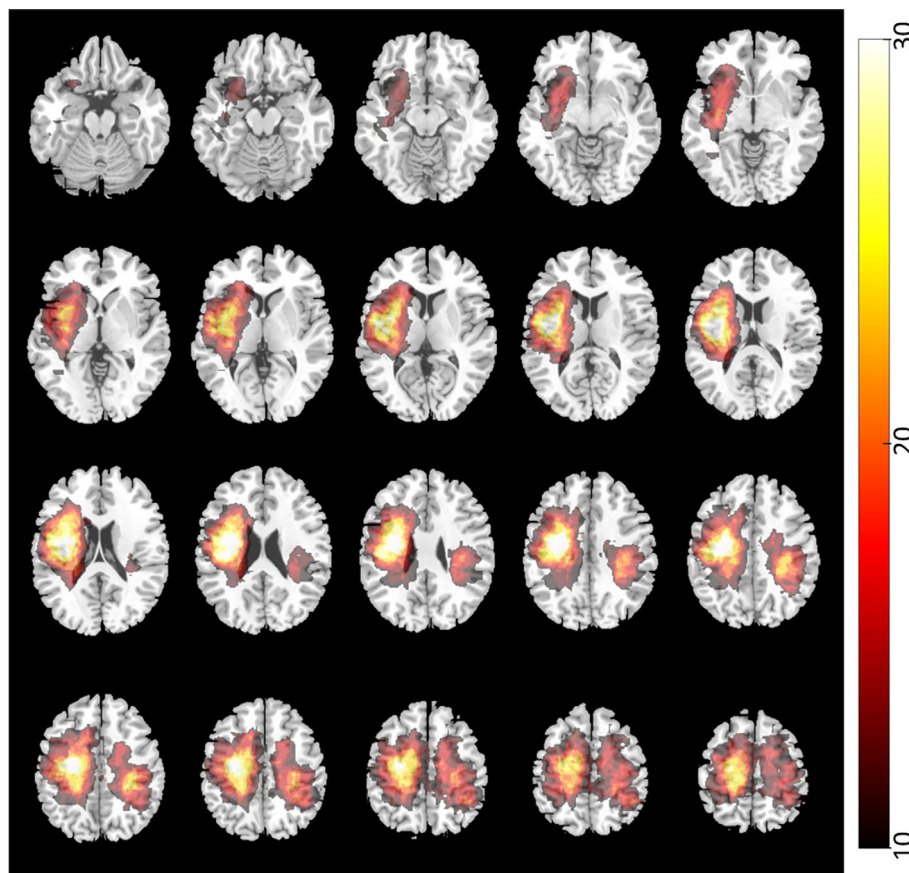
[a]Values are means ± standard error of mean.

FIGURE 3 Results of tumor overlapping. The number in the color bar represented the number of gliomas with same locations

X_r, Y_r, and Z_r, and for point T, the points located on the tumor border are represented by X_t, Y_t, and Z_t. The shortest distance is represented by D.

$$D = \sqrt{(X_r - X_t)^2 + (Y_r - Y_t)^2 + (Z_r - Z_t)^2}.$$

The correlation between the SDTN and AQ was analyzed. In the causal mediation analysis, each topological property was an independent variable, the mediator was the SDTN, and the AQ was the dependent variable.

3 | RESULTS

Ninety right-handed patients met the inclusion criteria and were ultimately included in our analysis. There were no differences in sex, age, or education level (Table 1). Based on the WAB results, all patients were classified into the aphasia ($n = 21$), MA ($n = 28$), and normal ($n = 41$) groups according to their preoperative language performance scores. Language performance differed among the three groups ($p < .0001$, one-way ANOVA test), and the post hoc analysis with Sidak correction revealed lower scores in the aphasia group compared with the MA ($p < .0001$) and normal ($p < .0001$) groups.

Moreover, the SDTN differed among the three groups ($p < .0001$, one-way ANOVA). After Sidak correction, the SDTN was shorter in the aphasia group compared with that in the MA ($p = .0080$) and normal ($p < .0001$) groups. Moreover, the SDTN was shorter in the MA group compared with that in the normal group ($p = .0434$). No differences in tumor volume were found among the three groups (Figure 3).

3.1 | Global topological differences in the language network

Global efficiency ($p = .0224$), local efficiency ($p = .0206$), shortest path length ($p = .0023$), and vulnerability ($p = .0209$) were significantly different among the three groups, as demonstrated by one-way ANOVA (Figure 4; Table S3).

Post hoc analysis with Sidak correction showed that the shortest path length was decreased in the MA ($p = .0016$) and normal ($p = .0382$) groups compared with that in the aphasia group. Moreover, vulnerability was increased in the MA ($p = .0331$) and normal ($p = .0409$) groups compared with that in the aphasia group. The global efficiency was significantly lower in the aphasia group compared with that in the MA group ($p = .0179$). Moreover, the local efficiency was lower in the aphasia group compared with that in the MA group ($p = .0169$).
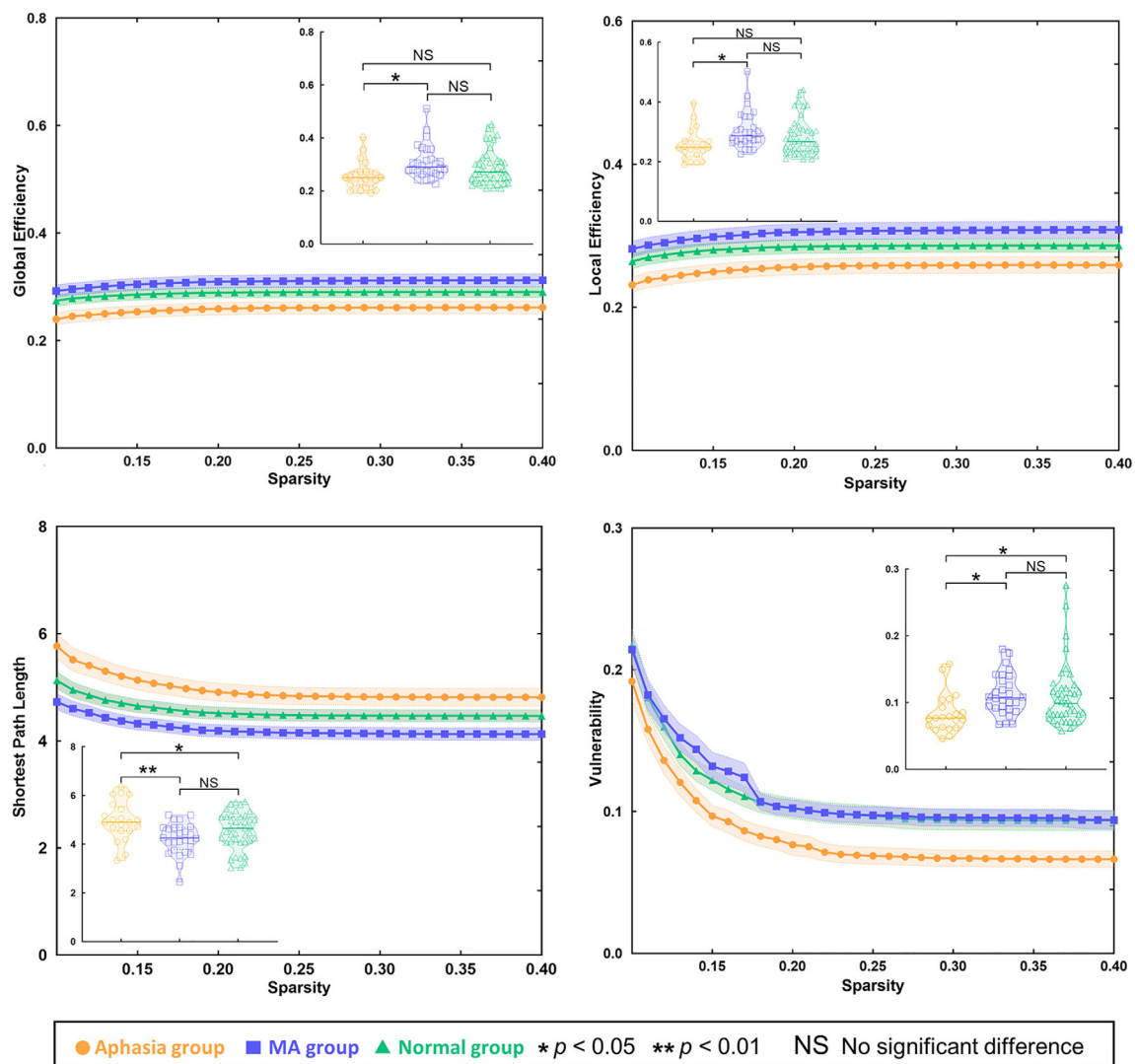
FIGURE 4 Alterations of global properties between the aphasia, MA, and normal groups. MA= mild anomia

3.2 | Nodal property differences in the language network

Regarding nodal efficiency (Figure 5; Table S4), the caudal BA 45 (pars triangularis; A45c_R, $p = .0034$), BA 41/42 (primary auditory cortex; A41/42_L, $p = .0333$), and caudal BA 22 (posterior superior temporal gyrus; A22c_R, $p = .0078$) were different among the three groups according to one-way ANOVA. Moreover, after post hoc analysis with Sidak correction, the nodal efficiency of node A45c_R in the MA group was higher than that in the aphasia ($p = .0037$) and normal ($p = .0379$) groups. Similarly, node A41/42_L showed increased nodal efficiency in the MA group compared with that in the aphasia ($p = .0378$) and normal groups ($p = .0020$). In addition, the nodal efficiency of node A22c_R in the MA group was higher than that in the aphasia ($p = .0049$) and normal ($p = .0064$) groups.

Nodal local efficiency (Table S5) of node A45c_R was significantly different among the three groups ($p = .0049$, one-way ANOVA). After post hoc analysis with Sidak correction, nodal local efficiency decreased in the MA ($p = .0046$) and normal ($p = .0299$) groups compared with that in the aphasia group.

The nodal degree centrality (Table S6) of node rostral BA 22 (A22r_R, $p = .0009$) was different among the three groups according to one-way ANOVA. After post hoc analysis with Sidak correction, the nodal degree centrality increased in the aphasia ($p = .0181$) and MA ($p = .0018$) groups compared with that in the normal group.

Furthermore, nodal clustering coefficients (Table S7) of the nodes A45c_R ($p < .0001$) and A41/42_L ($p = .0028$) were significantly different among the three groups based on one-way ANOVA. After post hoc analysis with Sidak correction, the nodal clustering coefficient of node A45c_R increased in the aphasia group compared with that in the MA ($p < .0001$) and normal ($p = .0002$) groups. In addition, the nodal clustering coefficient of node A41/42_L was higher in the aphasia group than that in the MA ($p = .0041$) and normal ($p = .0092$) groups. The remaining results are provided in the supplementary materials (Table S8).
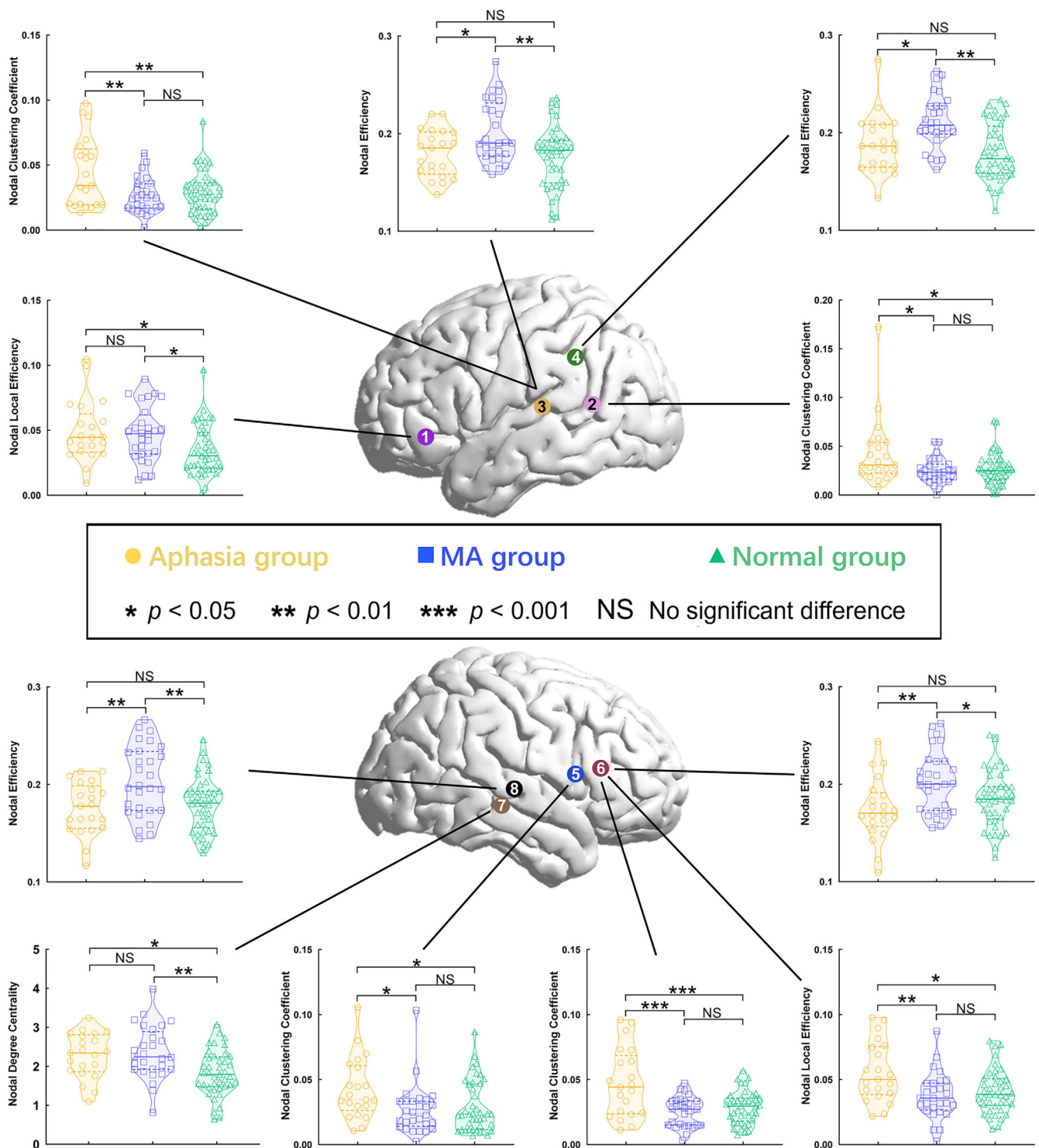
FIGURE 5 Alterations of nodal properties between the aphasia, MA, and normal groups. The upper panel showed the altered nodes that were located in the left hemisphere. Purple node (no. 1) = rostral BA 45. Pink node (no. 2) = caudal posterior superior temporal sulcus. Orange node (no. 3) = BA 41/42. Green node (no. 4) = caudal BA 40. The inferior panel showed the altered nodes that were located in the right hemisphere. Blue node (no. 5) = ventral BA 44. Red node (no. 6) = caudal BA 45. Brown node (no. 7) = rostral BA 22. Black node (no. 8) = caudal BA 22. BA = Brodmann area. MA = mild anomia

3.3 | Correlation analysis

Results of the correlation analysis between AQs, topological properties, and the SDTN are shown in Figure 6. Nodal efficiency (r = 0.292,

p = .0418) and nodal vulnerability (r = 0.292, p = . 0419) of the node A22c_R were positively correlated with AQs. Moreover, the nodal clustering coefficient of this node (r = −0.327, p = .0218), the nodal degree centrality of the left rostroventral BA 39 (angular gyrus;
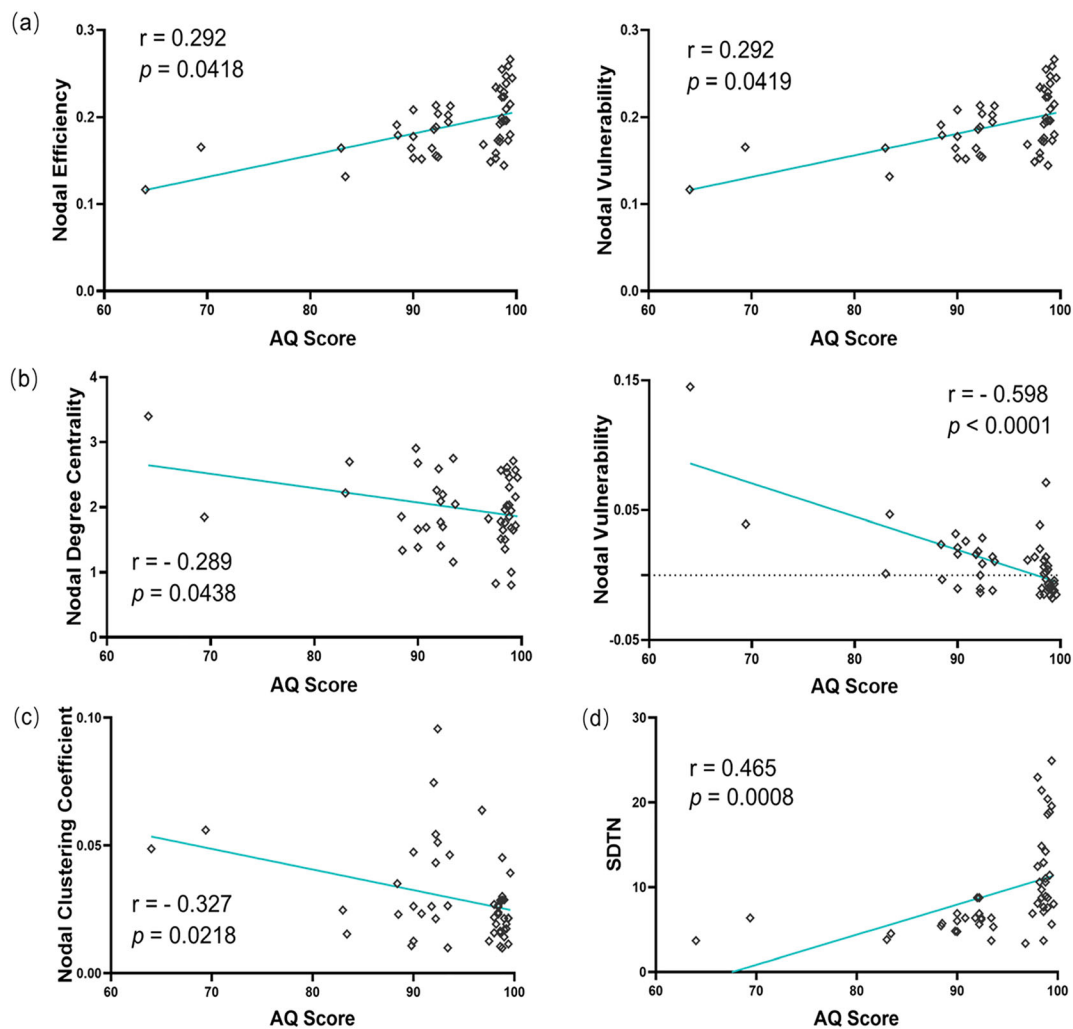
FIGURE 6 Pearson's correlation analysis between AQs and nodal topological properties in the aphasia and MA groups (n = 49). (a) Nodal efficiency and vulnerability of node A22c_R were positively correlated with AQs. (b) Nodal degree centrality and vulnerability of node A39rv_L was negatively correlated with AQs. (c) Nodal clustering coefficient of node A22c_R was negatively correlated with AQs. (d) SDTN was positively correlated with AQs. AQ = aphasia quotient; SDTN = the shortest distance from the tumor to the language network.

A39rv_L, r = −0.289, p = .0438), and nodal vulnerability of node A39rv_L (r = −0.598, p < .0001) were all negatively correlated with AQs. Furthermore, the SDTN was significantly positively correlated with AQs (r = 0.465, p = .0008).

3.4 | Causal mediation results

Regarding nodal degree centrality (total effect = −5.84, DE = −4.22, IE = −1.62, DE% = 72.26%, IE% = 27.74%; Figure S5a; Table S9) and nodal vulnerability (total effect = −177.68, DE = −154.47, IE = −23.20, DE% = 86.94%, IE% = 13.06%; Figure S5b; Table S10) of node A39rv_L, the SDTN was a mediating factor that affected the AQs.

4 | DISCUSSION

In this study, our results indicated that a decrease in the shortest path length of the language network helped to avoid preoperative language

deficit. Moreover, patients with a glioma that was closer to the language network had worse preoperative language performance. Furthermore, some nodes in the language network participated in compensation of language deficits located in the homotopic regions of the conventional Broca's and Wernicke's areas of the right hemisphere.

4.1 | Decreasing shortest path length and increasing vulnerability relate to avoiding language deficit

The shortest path length reflects the lowest energy cost of transmitting information through a network (Fang et al., 2020). An increase in the shortest path length indicates decreased efficiency of the network. Consistent with the findings of a previous study on patients with primary progressive aphasia (Agosta et al., 2014), our findings indicated that gliomas in the aphasia group caused the shortest path length to prolong, thereby decreasing the efficiency of information conveying could lead to impaired language function.

Vulnerability reflects the average alteration of global efficiency in a network when each node is removed in turn (Latora & Marchiori, 2005). Unlike previous findings in patients with stroke (specifically, increased vulnerability and simultaneously increased shortest path length) (de Lange et al., 2019; Guo et al., 2019), we found that patients with gliomas had increased vulnerability and decreased shortest path length. Different neurological disorders (specifically, stroke and gliomas) are related to different alterations in vulnerability and the shortest path length. Stroke is an acute disease that disrupts networks surrounding the lesion and causes problems with network reorganization (Guo et al., 2019; Zhu et al., 2016). Thus, after a person experiences stroke damage, performing a specific function must rely on the residual network with a longer shortest path length than that before the stroke occurred. However, glioma is a progressive disease that disrupts the original network, although it also provides sufficient time for the reorganization of the network (Cho et al., 2022; Tate et al., 2014). Hence, even if the glioma is located in the language network, the reorganized network maintains normal language functions.

4.2 | Tumor location reflects the degree of language function

Tumor location in the language eloquent area can predict the degree of dysfunction in future language performance (Yu et al., 2016; Zarino et al., 2021). Tumor location was found to be a risk predictor for language impairment (Fang, Liang, et al., 2021) by evaluating the distance from tumor to fibers (structural network). However, the role of the distance from the tumor to the functional network remained unknown. Our findings filled the gap in the literature and indicated that the SDTN had significant different among the three groups and was positively correlated with AQs. Moreover, our findings demonstrate that the SDTN is an important mediating factor for nodal degree centrality and nodal vulnerability of node A39rv_L that negatively affect the AQs. Furthermore, we observed no differences in tumor volumes among the three groups, which helped us to exclude tumor volume as a factor in language performance. Hence, the SDTN was an independent factor for preoperative language performance. Therefore, patients with a shorter SDTN may have worse language deficits since the language network is closer to the surgical area.

4.3 | Nodes in the language network at the nondominant hemisphere contribute to reorganization of the damaged language network

The mirrored side of the Broca's area in the right hemisphere plays an important role in reorganizing the damaged language network following stroke or other neurological disorders (Audrain et al., 2018; Skeide & Friederici, 2016; Thiel et al., 2006). Nodal efficiency represents the ability of information conveying of a node and calculates the efficiency of the sub-network in which the node is directly involved (Fang et al., 2020). Node A45c_R, as the right mirror side of the

Broca's area, had the highest nodal efficiency in the MA group in our study. This finding indicates that once the language network is affected, node A45c_R increases in response to language impairment, which explains why patients in the MA group had no aphasia. However, this site might not respond to the naming function because the MA group still showed a minor naming deficit. It seems plausible that this finding was related to the fact that Broca's area is conventionally thought to be associated with speech or pronunciation although not naming (Tate et al., 2014).

The mirrored Broca's and Wernicke's areas participate in reorganizing the damaged language network (Kertesz, 1993; Thiel et al., 2006). In our findings, different alterations in the adjacent cortex, A22c_R and A22r_R, corresponded to different levels of language performance (Mesulam et al., 2015). The node A22c_R relied on increasing nodal efficiency to help maintain the language ability of patients in the MA group. Moreover, the positive correlation between the nodal efficiency in A22c_R and the AQ was in line with the observation that node A22c_R could improve language performance in general although not naming ability. Accordingly, in node A22r_R, nodal degree centrality indicated that the impaired language network had higher connections with adjacent nodes to increase the importance of this node in both the aphasia and MA groups. The two groups were similar in having deficits in naming ability, although differed in the degree of the deficit. Hence, the nodal degree centrality in node A22r_R may be a marker of anomia. Overall, the findings of A22c_R and A22r_R confirm the compensatory ability of the posterior superior temporal gyrus in the right hemisphere and reveal the changes in specific nodal properties to determine which factor of the nodes accommodates language impairment.

4.4 | Nodes in the language network at the dominant hemisphere contribute to language deficit

The inferior parietal lobe plays a key role in language learning and processing (Barbeau et al., 2017). In this region, the nodal properties of node A39rv_L reflect the impairments of the language network caused by gliomas. Nodal degree centrality and nodal vulnerability refer to the important degree of a network (Audrain et al., 2018). The higher the nodal degree centrality and nodal vulnerability, the more crucial the node. Our findings indicate that when the importance of node A39rv_L increases, the AQs worsen. The sequence of network reorganization was initially located in the surrounding lesion, followed by the remote area in the ipsilateral hemisphere and the contralateral hemisphere with increased damage (Tate et al., 2014). In our study, because node A39rv_L surrounded the glioma but was not directly invaded, this node initially participated in network reorganization according to the classical theory of network reorganization (Herbet et al., 2016). Hence, the increased degree centrality and vulnerability of node A39rv_L in the language network may indicated that the degree of damage to language function induced by gliomas.

The main limitation of this study was that the SDTN only reflected the effect of the language network and did not reflect the

effect on a specific node because the node of the SDTN was not uniform. Due to our limited sample size of patients with different types of language deficits, we could not investigate the relationship between a specific node and specific type of language deficit. Moreover, the influences between ipsilateral and contralateral to the dominant hemisphere were not expanded in this study because of statistical power lack of data. In the future, studies that include more patients can fill these gaps.

5 | CONCLUSION

The shortest distance between the tumor and language network had a strong influence on the language performance of patients, and the aphasia and MA groups had differently altered nodes that compensated for the damaged language function. In summary, these findings suggest that the caudal BA 45 and caudal BA 22 in the right hemisphere and rostroventral BA 39 in the left hemisphere should be protected during surgery to preserve the plasticity of the language network to repair language ability postoperatively.

CONFLICT OF INTEREST
The authors report no competing interests.

DATA AVAILABILITY STATEMENT
Due to privacy issues related to clinical data, the anonymized data will be made available on request. The request should include a formal project outline for approval by the authors' local ethics committee.

ORCID
Tao Jiang https://orcid.org/0000-0001-7031-7773

REFERENCES
Agosta, F., Galantucci, S., Valsasina, P., Canu, E., Meani, A., Marcone, A., Magnani, G., Falini, A., Comi, G., & Filippi, M. (2014). Disrupted brain connectome in semantic variant of primary progressive aphasia. *Neurobiology of Aging*, *35*(11), 2646–2655. https://doi.org/10.1016/j.neurobiolaging.2014.05.017

Audrain, S., Barnett, A. J., & McAndrews, M. P. (2018). Language network measures at rest indicate individual differences in naming decline after anterior temporal lobe resection. *Human Brain Mapping*, *39*(11), 4404–4419. https://doi.org/10.1002/hbm.24281

Barbeau, E. B., Chai, X. J., Chen, J. K., Soles, J., Berken, J., Baum, S., Watkins, K. E., & Klein, D. (2017). The role of the left inferior parietal lobule in second language learning: An intensive language training fMRI study. *Neuropsychologia*, *98*, 169–176. https://doi.org/10.1016/j.neuropsychologia.2016.10.003

Biswal, B., Yetkin, F. Z., Haughton, V. M., & Hyde, J. S. (1995). Functional connectivity in the motor cortex of resting human brain using echo-planar MRI. *Magnetic Resonance in Medicine*, *34*(4), 537–541. http://www.ncbi.nlm.nih.gov/pubmed/8524021

Briganti, C., Sestieri, C., Mattei, P. A., Esposito, R., Galzio, R. J., Tartaro, A., Romani, G. L., & Caulo, M. (2012). Reorganization of functional connectivity of the language network in patients with brain gliomas. *AJNR. American Journal of Neuroradiology*, *33*(10), 1983–1990. https://doi.org/10.3174/ajnr.A3064

Calhoun, V. D., Wager, T. D., Krishnan, A., Rosch, K. S., Seymour, K. E., Nebel, M. B., Mostofsky, S. H., Nyalakanai, P., & Kiehl, K. (2017). The impact of T1 versus EPI spatial normalization templates for fMRI data analyses. *Human Brain Mapping*, *38*(11), 5331–5342. https://doi.org/10.1002/hbm.23737

Chen, Q., Lv, H., Wang, Z., Wei, X., Liu, J., Liu, F., Zhao, P., Yang, Z., Gong, S., & Wang, Z. (2022). Distinct brain structural-functional network topological coupling explains different outcomes in tinnitus patients treated with sound therapy. *Human Brain Mapping*, *43*, 3245–3256. https://doi.org/10.1002/hbm.25848

Cho, N. S., Peck, K. K., Gene, M. N., Jenabi, M., & Holodny, A. I. (2022). Resting-state functional MRI language network connectivity differences in patients with brain tumors: Exploration of the cerebellum and contralesional hemisphere. *Brain Imaging and Behavior.*, *16*, 252–262. https://doi.org/10.1007/s11682-021-00498-5

Cirillo, S., Caulo, M., Pieri, V., Falini, A., & Castellano, A. (2019). Role of functional imaging techniques to assess motor and language cortical plasticity in glioma patients: A systematic review. *Neural Plasticity*, *2019*, 4056436–4056416. https://doi.org/10.1155/2019/4056436

Clark, H. M., Utianski, R. L., Duffy, J. R., Strand, E. A., Botha, H., Josephs, K. A., & Whitwell, J. L. (2020). Western aphasia battery-revised profiles in primary progressive aphasia and primary progressive apraxia of speech. *American Journal of Speech-Language Pathology*, *29*(1S), 498–510. https://doi.org/10.1044/2019_AJSLP-CAC48-18-0217

de Lange, S. C., Scholtens, L. H., van den Berg, L. H., Boks, M. P., Bozzali, M., Cahn, W., Dannlowski, U., Durston, S., Geuze, E., van Haren, N. E. M., Hillegers, M. H. J., Koch, K., Jurado, M. A., Mancini, M., Marques-Iturria, I., Meinert, S., Ophoff, R. A., Reess, T. J., Repple, J., Kahn, R. S., & van den Heuvel, M. P. (2019). Alzheimer's Disease Neuroimaging, I. Shared vulnerability for connectome alterations across psychiatric and neurological brain disorders. *Nature Human Behaviour*, *3*(9), 988–998. https://doi.org/10.1038/s41562-019-0659-6

Duffau, H. (2014). The huge plastic potential of adult brain and the role of connectomics: New insights provided by serial mappings in glioma surgery. *Cortex*, *58*, 325–337. https://doi.org/10.1016/j.cortex.2013.08.005

Fan, L., Li, H., Zhuo, J., Zhang, Y., Wang, J., Chen, L., Yang, Z., Chu, C., Xie, S., Laird, A. R., Fox, P. T., Eickhoff, S. B., Yu, C., & Jiang, T. (2016). The human Brainnetome atlas: A new brain atlas based on connectional architecture. *Cerebral Cortex*, *26*(8), 3508–3526. https://doi.org/10.1093/cercor/bhw157

Fang, S., Liang, Y., Li, L., Wang, L., Fan, X., Wang, Y., & Jiang, T. (2021). Tumor location-based classification of surgery-related language impairments in patients with glioma. *Journal of Neuro-Oncology*, *155*(2), 143–152. https://doi.org/10.1007/s11060-021-03858-9

Fang, S., Wang, Y., & Jiang, T. (2021). Epilepsy enhance global efficiency of language networks in right temporal lobe gliomas. *CNS Neuroscience & Therapeutics*, *27*(3), 363–371. https://doi.org/10.1111/cns.13595

Fang, S., Zhou, C., Fan, X., Jiang, T., & Wang, Y. (2020). Epilepsy-related brain network alterations in patients with temporal lobe glioma in the left hemisphere. *Frontiers in Neurology*, *11*, 684. https://doi.org/10.3389/fneur.2020.00684

Fang, S., Zhou, C., Wang, Y., & Jiang, T. (2021). Contralesional functional network reorganization of the insular cortex in diffuse low-grade glioma patients. *Scientific Reports*, *11*(1), 623. https://doi.org/10.1038/s41598-020-79845-3

Forkel, S. J., Thiebaut de Schotten, M., Dell'Acqua, F., Kalra, L., Murphy, D. G., Williams, S. C., & Catani, M. (2014). Anatomical predictors of aphasia recovery: A tractography study of bilateral perisylvian language networks. *Brain*, *137*(Pt 7), 2027–2039. https://doi.org/10.1093/brain/awu113

Guo, X., Simas, T., Lai, M. C., Lombardo, M. V., Chakrabarti, B., Ruigrok, A. N. V., Bullmore, E. T., Baron-Cohen, S., Chen, H., Suckling, J., & Consortium, M. A. (2019). Enhancement of indirect functional connections with shortest path length in the adult autistic brain. *Human Brain Mapping*, *40*(18), 5354–5369. https://doi.org/10.1002/hbm.24777

Herbet, G., Maheu, M., Costi, E., Lafargue, G., & Duffau, H. (2016). Mapping neuroplastic potential in brain-damaged patients. *Brain*, *139*(Pt 3), 829–844. https://doi.org/10.1093/brain/awv394

Kertesz, A., Lau, W. K., & Polk, M. (1993). Recovery from wernicke's aphasia: A positron emission tomographic study. *Brain and language*, *44*(2), 153-164.

Kertesz, A., & Poole, E. (1974). The aphasia quotient: The taxonomic approach to measurement of aphasic disability. *Canadian Journal of Neurological Sciences/Journal Canadien des Sciences Neurologiques*, *1*(1), 7–16. https://doi.org/10.1017/s031716710001951x

Latora, V., & Marchiori, M. (2005). Vulnerability and protection of infrastructure networks. *Physical Review. E, Statistical, Nonlinear, and Soft Matter Physics*, *71*(1 Pt 2), 015103. https://doi.org/10.1103/PhysRevE.71.015103

Liu, Y., Liang, M., Zhou, Y., He, Y., Hao, Y., Song, M., Yu, C., Liu, H., Liu, Z., & Jiang, T. (2008). Disrupted small-world networks in schizophrenia. *Brain*, *131*(Pt 4), 945–961. https://doi.org/10.1093/brain/awn018

Mesulam, M. M., Thompson, C. K., Weintraub, S., & Rogalski, E. J. (2015). The Wernicke conundrum and the anatomy of language comprehension in primary progressive aphasia. *Brain*, *138*(Pt 8), 2423–2437. https://doi.org/10.1093/brain/awv154

Plaza, M., Gatignol, P., Leroy, M., & Duffau, H. (2009). Speaking without Broca's area after tumor resection. *Neurocase*, *15*(4), 294–310. https://doi.org/10.1080/13554790902729473

Satoer, D., Visch-Brink, E., Smits, M., Kloet, A., Looman, C., Dirven, C., & Vincent, A. (2014). Long-term evaluation of cognition after glioma surgery in eloquent areas. *Journal of Neuro-Oncology*, *116*(1), 153–160. https://doi.org/10.1007/s11060-013-1275-3

Skeide, M. A., & Friederici, A. D. (2016). The ontogeny of the cortical language network. *Nature Reviews. Neuroscience*, *17*(5), 323–332. https://doi.org/10.1038/nrn.2016.23

Tate, M. C., Herbet, G., Moritz-Gasser, S., Tate, J. E., & Duffau, H. (2014). Probabilistic map of critical functional regions of the human cerebral cortex: Broca's area revisited. *Brain*, *137*(Pt 10), 2773–2782. https://doi.org/10.1093/brain/awu168

Thiel, A., Habedank, B., Herholz, K., Kessler, J., Winhuisen, L., Haupt, W. F., & Heiss, W. D. (2006). From the left to the right: How the brain compensates progressive loss of language function. *Brain and Language*, *98*(1), 57–65. https://doi.org/10.1016/j.bandl.2006.01.007

Tuncer, M. S., Salvati, L. F., Grittner, U., Hardt, J., Schilling, R., Bahrend, I., Silva, L. L., Fekonja, L. S., Faust, K., Vajkoczy, P., Rosenstock, T., & Picht, T. (2021). Towards a tractography-based risk stratification model for language area associated gliomas. *Neuroimage Clinical*, *29*, 102541. https://doi.org/10.1016/j.nicl.2020.102541

Yu, Z., Tao, L., Qian, Z., Wu, J., Liu, H., Yu, Y., Song, J., Wang, S., & Sun, J. (2016). Altered brain anatomical networks and disturbed connection density in brain tumor patients revealed by diffusion tensor tractography. *International Journal of Computer Assisted Radiology and Surgery*, *11*(11), 2007–2019. https://doi.org/10.1007/s11548-015-1330-y

Yuan, B., Zhang, N., Yan, J., Cheng, J., Lu, J., & Wu, J. (2019). Resting-state functional connectivity predicts individual language impairment of patients with left hemispheric gliomas involving language network. *Neuroimage Clinical*, *24*, 102023. https://doi.org/10.1016/j.nicl.2019.102023

Zarino, B., Sirtori, M. A., Meschini, T., Bertani, G. A., Caroli, M., Bana, C., Borellini, L., Locatelli, M., & Carrabba, G. (2021). Insular lobe surgery and cognitive impairment in gliomas operated with intraoperative neurophysiological monitoring. *Acta Neurochirurgica*, *163*(5), 1279–1289. https://doi.org/10.1007/s00701-020-04643-9

Zhang, H., Ille, S., Sogerer, L., Schwendner, M., Schroder, A., Meyer, B., Wiestler, B., & Krieg, S. M. (2021). Elucidating the structural-functional connectome of language in glioma-induced aphasia using nTMS and DTI. *Human Brain Mapping*, *43*, 1836–1849. https://doi.org/10.1002/hbm.25757

Zhu, Y., Bai, L., Liang, P., Kang, S., Gao, H., & Yang, H. (2016). Disrupted brain connectivity networks in acute ischemic stroke patients. *Brain Imaging and Behavior*, *11*(2), 444–453. https://doi.org/10.1007/s11682-016-9525-6

SUPPORTING INFORMATION

Additional supporting information can be found online in the Supporting Information section at the end of this article.